Prabha Materials Science Letters
Vol. 5, No. 2, 286-307, 2026
https://doi.org/10.33889/PMSL.2026.5.2.016

Averting Microstructural Inhomogeneities: A Probabilistic Framework for Elastic Modulus Prediction in Metal Matrix Nanocomposites

Sanjay Gupta
Department of Mechanical Engineering,
Netaji Subhas University of Technology, Sector 3, Dwarka, 110078, New Delhi, India.
E-mail: sgupta@nsut.ac.in

Abhishek Tevatia
Department of Mechanical Engineering,
Netaji Subhas University of Technology, Sector 3, Dwarka, 110078, New Delhi, India.
Corresponding author: abhishek.tevatia@nsut.ac.in

K. P. S. Rana
Department of Instrumentation and Control Engineering,
Netaji Subhas University of Technology, Sector 3, Dwarka, 110078, New Delhi, India.
E-mail: kpsrana@nsut.ac.in

(Received on October 14, 2025; Revised on April 19, 2026 & May 14, 2026; Accepted on May 30, 2026)

Abstract
In this article, a comprehensive study of the elastic modulus of metal matrix nanocomposites (MMNCs) that accounts systematically the influence of the presence of pores and aggregates of nanoparticles. A very effective micromechanical modelling technique was developed. The empirical correlations described the controlling effects of the microstructural features on the stiffness reduction in terms of numbers. The results of the study show that the porosity as well as the clustering of particles, both reduce the effective elastic modulus significantly, primarily due to the increased stress concentration zones and reduction in load transfer paths. The model is checked using the models and data sets used in the experiments. It has been shown to have high prediction accuracy for a broad spectrum of MMNC formulations. In order to cope with the inherent material variability a complementary probabilistic assessment was conducted. Monte Carlo simulations, empirical cumulative distribution functions (ECDFs) and reliability assessments were used to statistically distribute the effective modulus values. The analysis estimates the probabilities of reaching design goals and systematically correlates the dispersion of the modulus with failure probabilities. In this study, a deterministic model and a probabilistic risk analysis are performed together, aiming to present a reliable and performance-oriented framework for the design of MMNCs which was applied to an advanced structural system. The presented combined deterministic and probabilistic framework is realistic and risk-informed and serves as a basis for the structural design of the high performance MMNCs, thus moving the material reliability towards critical applications.

Keywords- Metal matrix nanocomposites (MMNCs), Elastic modulus, Porosity, Nanoparticle agglomeration, Micromechanical modelling, Probabilistic analysis.

1. Introduction

The requirement of lightweight and high-strength materials in the field of advanced engineering, such as aerospace and defense, has resulted in a considerable increase in the development and application of MMNCs (Zhang & Xu, 2022). These advanced structural systems are characterized by the combination of nanoscale ceramic particles (≤ 100 nm) such as Al_2O_3, SiC and TiC with metallic matrices such as aluminum and magnesium. Such microstructural engineering results in significant improvements in mechanical, thermal and tribological properties making MMNCs as potential candidates for next generation material solutions (Ceschini et al., 2017; Dahiya et al., 2023; Gupta et al., 2022, 2025; He et al., 2008).

The elastic modulus is an important parameter of mechanical performance, which is the measure of macroscopic stiffness and structural integrity in the harsh conditions of load-bearing (Ceschini et al., 2017; Hassan & Gupta, 2006). However, the realization of these theoretically idealized behaviors is often limited by microstructural variability. It has been demonstrated through empirical research and simulation-based reconstruction that the intrinsic manufacturing complexities (Abdizadeh et al., 2014; Rana et al., 2012) induce the porosity (Ahmad et al., 2007; Brassell et al., 1975; Mirza & Chen, 2012) and nanoparticle agglomeration (Hassanzadeh-Aghdam et al., 2018; Mazaheri et al., 2024; Pan & Bian, 2019; Pouyanmehr et al., 2022), leading to spatially heterogeneous regions of mechanical weakness, variation in stiffness and fluctuations in local strength.

Hence, probabilistic variations in microstructure, such as the presence of stochastic distributions of reinforcement and imperfect interfaces cannot be resolved accurately through conventional deterministic approaches and pose a challenge for the modeling and predictive assessment of MMNCs. The standard micromechanical models are only based on the idealized assumptions of homogeneity and interface cohesion (Baxter & Robinson, 2011; Hassan & Gupta, 2004; Hsu et al., 2006; Mortazavi et al., 2013; Nayak et al., 2010; Snipes et al., 2011; Yang & Meng, 2026). These restrictions limit the ability to predict macroscopic properties from microstructural heterogeneities reliably and emphasize the need for advanced statistical and stochastic modeling techniques capable of capturing the variability and overall trends of real-life MMNC architectures.

For these reasons, probabilistic modelling has been adopted as a useful tool for composite materials, to account for uncertainties in the microstructure and property prediction problem (Engelstad & Reddy, 1994; McWilliams et al., 2013; Rapoff et al., 1999; Shah et al., 2000; Zhao et al., 2022). These types of models assume that such microstructural characteristics as reinforcement distribution, the bonding strength of the interface and porosity levels can be assumed as random variables with statistical distributions. The variations of the elastic modulus of fibrous tissues have been dealt with by considering the microstructural features as independent random variables for a probabilistic rule of mixtures proposed by Rapoff et al. (1999). The Monte Carlo simulation method has also been used by Zhao et al. (2022) to study the effect of the randomness in reinforcement volume on the elastic modulus of particulate composites. These methodologies can also be used to increase the predictiveness and to gain insight into the uncertainty of that prediction and thereby increase the capability for risk-informed material design, a critical requirement for applications in engineering where consistency and reliability are paramount.

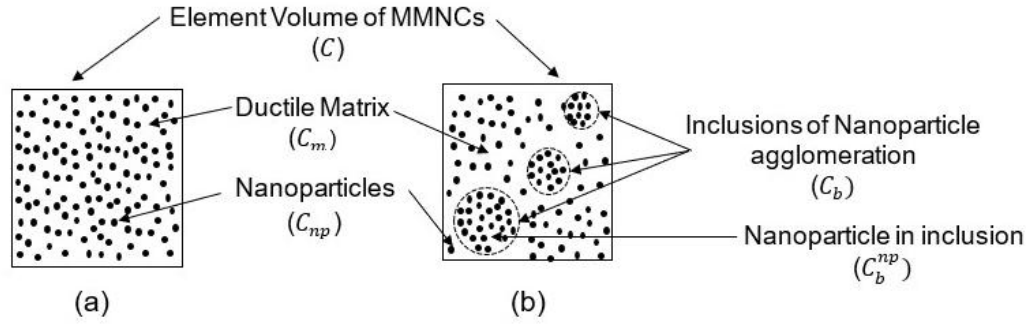

Figure 1. Illustration of element volume of MMNCs with (a) uniformly distributed (b) non-uniformly distributed (agglomerated) nanoparticles.

Porosity is one of the most important defects in the metal matrix nanocomposites (MMNCs) mainly due to the processing techniques like powder metallurgy and stir casting (Mirza & Chen, 2012). Voids are stress concentrators that reduce the load-bearing cross-section and degrade the mechanical properties (Ahmad et al., 2005; Ahmad et al., 2007; Brassell et al., 1975; Mirza & Chen, 2012; Molina et al., 2009). The spherical pores and gas porosity are responsible for the failure initiation by creating stress concentration problems. The properties of MMNCs such as ductility and stiffness are dependent on the load bearing reinforcement particles and voids (Ahmad et al., 2005). The presence of a large number of small voids, formed due to oxides, surrounded by single or clusters of reinforcing particles considerably deteriorates the mechanical and thermal properties of MMNCs (Sahoo et al., 2021). Therefore, the effect of porosity especially in the presence of nanoparticles is of extreme importance as it may deteriorate the porosity levels in MMNCs. Agglomeration of nanoparticles is another common problem in the fabrication of MMNCs.

Non-uniform dispersion and distribution of nanoscale reinforcements within the composite matrix leads to agglomeration or clustering of nanoparticles (Mazaheri et al., 2024; Pan & Bian, 2017; Pouyanmehr et al., 2022). These clusters act as mechanically weak spots, disrupt load transfer and increase the heterogeneity of the mechanical response. Agglomeration variations (**Figure 1b**) are the process by which weakly coupled particles are formed into strong and dense clusters that are susceptible to disruption by mechanical forces (Pan & Bian, 2019). During MMNC manufacture, the nanoparticle agglomeration is caused by electrostatic interactions and high particle surface energy (Pan & Bian, 2017). The effect of agglomeration in nanocomposites has been studied by several researchers (Golbang et al., 2017; Karevan et al., 2010; Pan & Bian, 2017, 2019; Pouyanmehr et al., 2022; Qiao et al., 2011; Shi et al., 2004; Zare, 2016). These studies concluded that agglomeration leads to the formation of high-stress regions and defects in nanocomposites, which in turn decreases mechanical properties like elastic modulus, yield strength, and hardness of MMNCs.

The main microstructural inhomogeneities such as porosity and nanoparticle agglomeration collectively reduce the average mechanical properties of MMNCs and generate large statistical fluctuations in key properties. The synergistic interactions between these factors further complicate the mechanical properties. Agglomeration promotes porosity and increasing porosity increases interfacial debonding This demonstrates the need for integrated probabilistic modelling methodologies. In this study, a thorough probabilistic framework is proposed for the characterisation of elastic modulus of MMNCs considering measurable impacts of porosity, nanoparticle agglomeration and reinforcement volume fraction. The present model does not explicitly take into account the effects of interfacial debonding. The framework considers empirical degradation and clustering coefficients as stochastic variables and thus captures the statistical dispersion of such inhomogeneities in the real world and its cumulative effect on the composite performance. A systematic sensitivity analysis was carried out to clarify the effect of uncertainties of parameters on the predicted stiffness, which enables to identify the dominant degradation mechanisms and the main contributors to the modeling uncertainty. The probabilistic approach accounts for the uncertainty in particle dispersion and clustering, which the deterministic models do not. Multiple microstructure realizations improve spatial inhomogeneity and material behavior to address stochastic variability. Quantifying uncertainty in the effective elastic modulus is key to informed material design, and this paradigm provides mean responses and statistical distributions for improved predictions.

2. Predictive Modeling of Elastic Modulus

The addition of high modulus nanoparticles in MMNCs leads to a remarkable increase in their elastic modulus. The enhancement is due to the interaction of the microstructural parameters such as particle volume fraction, morphology, orientation, aspect ratio and porosity (Ceschini et al., 2017). At the macroscopic level, intrinsic properties of the matrix and reinforcement, processing route, thermomechanical

history, and interfacial bonding are important determinants of the ultimate performance of MMNCs (Abdizadeh et al., 2014; Rana et al., 2012).

Several micromechanical models have been developed to predict the scaling of the elastic modulus with particle loading, such as Eshelby's inclusion theory, Halpin-Tsai relations, the rule of mixtures, Mori-Tanaka schemes and finite-element unit cell methods (Baxter & Robinson, 2011; Hassan & Gupta, 2004; Hsu et al., 2006; Mortazavi et al., 2013; Nayak et al., 2010; Snipes et al., 2011). These models are computationally efficient but typically ignore the influence of nanoparticle size. However, in recent experimental studies, it was found that the modulus enhancement was strongly dependent on the dimension of the particles and smaller nanoparticles offered better reinforcement (El-Kady & Fathy, 2014; Gupta & Wong, 2015; Yao et al., 2017). A model for prediction of elastic modulus of particulate reinforced metal matrix composites has been proposed by Mital et al. (1997) and can be written as follows:

$$E_c = \frac{V_p^{\frac{2}{3}} E_m}{1 - V_p^{\frac{1}{3}}\left(1 - \frac{E_m}{E_p}\right)} + \left(1 - V_p^{\frac{2}{3}}\right) E_m \tag{1}$$

where, V_p is the particle volume fraction, and E_m, E_p are the elastic moduli of the matrix and particles.

Hassanzadeh-Aghdam et al. (2018), later extended this by introducing a size-efficiency factor φ_o, yielding:

$$E'_{nc} = \frac{\varphi_o V_{np}^{\frac{2}{3}} E_m}{1 - V_{np}^{\frac{1}{3}}\left(1 - \frac{E_m}{E_{np}}\right)} + \left(1 - V_{np}^{\frac{2}{3}}\right) E_m \tag{2}$$

with V_{np} as the nanoparticle volume fraction, E_{np} the nanoparticle modulus, and the size-efficiency factor φ_o is expressed as:

$$\varphi_o = 1 + \zeta . exp\left[\left(\frac{d_{np}}{d_{ref}}\right)^a\right] \tag{3}$$

where, ζ and an are material constants, d_{np} is the particle diameter (in nm) and the reference length is taken as $d_{ref} = 1\,nm$ for dimensional consistency. In this form, φ_o is maximum at $d_{np} \to 0$. This is characteristic of higher surface area to volume ratio and interfacial load transfer for smaller nanoparticles. However, for larger particle size the exponential term decreases and $\varphi_o \to 1$ and the classical composite response is recovered.

The material parameters ζ and an are calibrated to experimental data sets for metal matrix nanocomposites. Here, zeta is the magnitude of reinforcement enhancement, while a governs the sensitivity to particle size. Typical values of ζ are in the range 0.2–0.8 and a is in the range 0.5–2.0 for different material systems and interface characteristics (Chen et al., 2018; Hassanzadeh-Aghdam et al., 2018) obtained by regression analysis of available data.

The efficiency factor φ_o reflects the crucial role of particle size in strengthening MMNCs. Smaller nanoparticles with high surface to volume ratio will promote better matrix bonding and stress transfer However, excessive reduction may result in agglomeration and excessive interfacial area, which may affect the structural uniformity. Therefore, MMNCs often suffer from porosity and particle agglomeration due to processing constraints, despite their promising mechanical performance.

2.1 Influence of Porosity on Elastic Modulus

An accurate modeling of the elastic modulus of MMNCs should take into account the influence of microstructural defects, especially porosity. Pores can be formed by several mechanisms, for example gas trapping during solidification, poor interfacial bonding due to inadequate wetting of the reinforcement particles, or hydrogen evolution during the fabrication processes (Ceschini et al., 2017; Sinha & Farhat, 2015; Zhong et al., 2007). This porosity degrades the mechanical performance by breaking the structural continuity and also by impeding the efficient stress transfer (Sinha & Farhat, 2015; Zhong et al., 2007).

A major effect of porosity is the reduction of the load sharing effectiveness between the matrix and the embedded nanoparticles, which directly reduces the stiffness and the strength of the composite (Ahmad et al., 2007; Molina et al., 2009). To quantify this effect, a porosity degradation factor, $f_{porosity}$ is introduced and is defined as follows (Mirza & Chen, 2012):

$$f_{porosity} = 1\, e^{-\phi V_{porosity}} \tag{4}$$

where, $V_{porosity}$ is the pore volume fraction and ϕ is an empirical constant that reflects pore morphology, orientation, and size distribution. For cylindrical pores inclined at 40°-90° relative to the loading axis, ϕ can be estimated as $\phi = \frac{0.405 L_{np}}{D_{np}} + \frac{0.318 D_{np}}{L_{np}} + 1.22$ (Brassell et al., 1975) with L_{np} and D_{np} representing nanoparticle length and diameter, respectively. In this study, the nanoparticles are approximated as cubic, yielding a constant value of ϕ =1.943.

By incorporating the degradation factor into the modulus expression, the effective elastic modulus of the nanocomposite, E_{nc}, is given as:

$$E_{nc} = E'_{nc}\left(1 - f_{porosity}\right) \tag{5}$$

where, E'_{nc} is the porosity-free modulus. This formulation captures the reduction in stiffness induced by porosity, thereby offering a more realistic assessment of MMNC mechanical response under applied loading.

2.2 Impact of Nanoparticle Agglomeration on Elastic Modulus

The spatial distribution of nanoparticles in the metal matrix is an important factor affecting the mechanical properties of MMNCs. However, nanoparticle clustering or agglomeration is a common problem in fabrication processes which, similar to porosity, is a major microstructural defect that reduces the stiffness and impairs the load transfer (Boostani et al., 2016; Liu & Bian, 2018). Consequently, it is essential to incorporate the effects of agglomeration in predictive models of MMNC behavior.

As depicted in **Figure 1a**, the representative elementary volume of the composite is defined, comprising two subregions:

$$C_{np} + C_m = C \tag{6}$$

where, C_{np} is the nanoparticle volume and C_m is the matrix volume free of nanoparticles. The nanoparticle volume fraction is:

$$V_{np} = \frac{C_{np}}{C} \tag{7}$$

and the corresponding matrix fraction is:

$$V_m = 1 - V_{np} \tag{8}$$

If clustering occurs (**Figure 1b**), the total agglomerated volume is denoted by C_b, while the uniformly distributed region is:

$$C_u = C - C_b \tag{9}$$

The nanoparticle volume inside agglomerates is C_b^{np}, and those in the uniform region are $C_u^{np} = C_{np} - C_b^{np}$.

Two descriptors are introduced to quantify agglomeration:

$$\xi_b = \frac{C_b}{C} \quad \& \quad \lambda_b = \frac{C_b^{np}}{C_{np}} \tag{10}$$

where, ξ_b is the agglomerated volume fraction, and λ_b is the proportion of nanoparticles inside clusters.

Using Equations (7) and (10), the nanoparticle fractions in clustered and uniform regions are given as:

$$V_{np}^{agg} = \frac{C_b^{np}}{C_b} = \frac{\lambda_b}{\xi_b} V_{np} \tag{11}$$

$$V_{np}^{uniform} = \frac{C_u^{np}}{C_u} = \frac{(C_{np} - C_b^{np})}{C - C_b} = \frac{(1-\lambda_b)}{(1-\xi_b)} V_{np} \tag{12}$$

The agglomeration descriptors were confined within physically permissible limits such that $0 \leq \xi_b, \lambda_b \leq 1$, while the local nanoparticle volume fractions satisfied $0 \leq V_{np}^{agg}, V_{np}^{uniform} \leq 1$. The fractions of agglomerated and uniformly dispersed nanoparticles were assessed using Equation (11) and (12). To avoid non-physical outcomes, admissibility conditions $\lambda_b V_{np} \leq \xi_b$ and $(1 - \lambda_b)V_{np} \leq (1 - \xi_b)$ were enforced throughout the Monte Carlo simulations. These simulations were carried out within the experimentally relevant reinforcement range $0 \leq V_{np} \leq 0.05$, while ξ_b and λ_b were sampled under the aforementioned constraints. Any parameter combinations that violated these conditions were automatically excluded through constraint-based rejection sampling.

To account for the influence of nanoparticle agglomeration on the elastic modulus model (Equation (13c)) use Equations (11) and (12) in Equation (5). The effective modulus of the clustered region is:

$$E'_{b,nc} = \frac{\varphi_o \left(V_{np}^{agg}\right)^{\frac{2}{3}} E_m}{1 - \left(V_{np}^{agg}\right)^{\frac{1}{3}} \left(1 - \frac{E_m}{E_{np}}\right)} + \left(1 - \left(V_{np}^{agg}\right)^{\frac{2}{3}}\right) E_m \tag{13a}$$

and for the uniform region:

$$E'_{u,nc} = \frac{\varphi_o \left(V_{np}^{uniform}\right)^{\frac{2}{3}} E_m}{1 - \left(V_{np}^{uniform}\right)^{\frac{1}{3}} \left(1 - \frac{E_m}{E_{np}}\right)} + \left(1 - \left(V_{np}^{uniform}\right)^{\frac{2}{3}}\right) E_m \tag{13b}$$

The combined agglomeration-modified modulus is:

$$E'_{agg,nc} = \xi_b E'_{b,nc} + (1 - \xi_b) E'_{u,nc} \tag{13c}$$

Finally, incorporating porosity effects (Equation (5)), the effective elastic modulus of the nanocomposite is expressed as:

$$E_{eff,nc} = E'_{agg,nc}\left(1 - f_{porosity}\right) \tag{14}$$

This relation provides a unified framework to predict the modulus of MMNCs by simultaneously accounting for nanoparticle agglomeration and porosity effects**,** thus yielding a more realistic evaluation of composite stiffness.

3. Probabilistic Modeling of Elastic Modulus

Deterministic models are crucial in predicting the elastic modulus of MMNCs. However, deterministic models tend to be insufficient in addressing the stochastic nature of the real manufacturing process and microstructural variability. In practical terms, MMNCs are characterized by different kinds of imperfections, including porosity and nanoparticle agglomeration, randomly distributed throughout the different scales and processing stages. These intrinsic uncertainties require a probabilistic Modelling framework to make more accurate and robust predictions of mechanical behavior (Altarabsheh et al., 2025).

The probabilistic framework combines statistical distributions with micromechanical models such that the elastic modulus can be modelled as a random variable affected by the inherent microstructural variations as shown in **Figure 2**. The volume fraction of nanoparticles, agglomeration intensity, and level of porosity are all key parameters that are characterized by using appropriate probability density functions (PDFs) that are obtained from empirical data or from reasonable assumptions based on processing conditions. The probabilistic model assumes that this modulus is a function of several stochastic variables, i.e.

$$E_{eff,nc} = f\left(V_{np}, d_{np}, \varphi_o, \xi_b, \lambda_b, V_{porosity}\right) \tag{15}$$

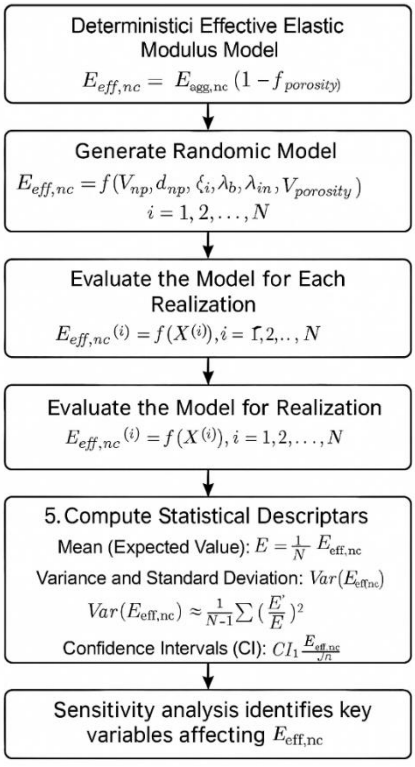

Figure 2. Flowchart of the probabilistic framework for estimating the effective elastic modulus of nanocomposites, including model generation, evaluation, statistical analysis, and sensitivity assessment.

Each input parameter is described by a distribution, i.e., normal, lognormal, or beta, depending on the physical range of the parameter and the variability of its measurement, as shown in **Table 1**.

Table 1. Probabilistic distribution of input variables used in elastic modulus modelling.

Parameter	Probability distribution	Mean / Nominal value	Standard deviation	Bounds	Description
V_{np}	Uniform / Normal $V_{np} \sim N(\mu, \sigma^2)$or Uniform (b)	0.025	—	0-0.05	Reflects controlled reinforcement input with known average or bounded experimental variability.
d_{np}(nm)	Normal / Uniform $d_{np} \sim N(\mu, \sigma^2)$or Uniform (b)	System-dependent (13-400 nm)	5% of mean	Positive values only	Represents measurable nanoparticle size with known average or bounded processing variability.
$V_{porosity}$	Lognormal $V_{porosity} \sim Lognormal(\mu, \sigma^2)$	0.01	0.002	$V_{porosity} \geq 0$	Porosity is strictly positive and generally exhibits right-skewed statistical behavior.
λ_b	Uniform / Normal $\lambda_b \sim N(\mu, \sigma^2)$or Uniform (b)	0.5	—	0-1	Represents the random fraction of nanoparticles located within agglomerated regions.
ξ_b	Uniform / Normal $\xi_b \sim N(\mu, \sigma^2)$or Uniform (b)	0.5	—	0-1	Models stochastic variability in the extent of nanoparticle clustering.
ϕ_o	Normal / Uniform $\phi_o \sim N(\mu, \sigma^2)$or Uniform (b)	Computed from Equation (3)	3% of mean	Positive values only	Depends on nanoparticle size and reinforcement efficiency; varies predictably with particle diameter.

3.1 Model Evaluation

The Monte Carlo simulation is a powerful statistical tool to quantify the uncertainty of the prediction of the effective elastic modulus of MMNCs. Unlike deterministic methods that provide only one output, the Monte Carlo method considers the stochasticity of the key input variables, i.e., the nanoparticle volume fraction, particle diameter, porosity, and agglomeration characteristics, by treating them as random variables from a given probability distribution (Engelstad & Reddy, 1994; McWilliams et al., 2013; Rapoff et al., 1999; Shah et al., 2000; Zhao et al., 2022).

The procedure begins with the development of a mathematical model in which the elastic modulus is expressed as a multivariate function of these stochastic inputs, as presented in Equation (17). For each iteration of the simulation many samples of random inputs are generated to capture variability in the model parameters. We denote the number of Monte Carlo samples, usually large (e.g. $N = 10^4$), to achieve statistical convergence. For each sample *i*, a realization of the entire input vector is constructed. This vector, called $X(i)$, contains all relevant microstructural variables considered as random:

$$X(i) = f\left(V_{np}^{(i)}, d_{np}^{(i)}, \varphi_o^{(i)}, \xi_b^{(i)}, \lambda_b^{(i)}, V_{porosity}^{(i)}\right), \qquad i = 1, 2, 3, \dots, N \tag{16}$$

Each component of this vector is sampled independently from the probability distribution given in **Table 1**. This sampling provides a representative population of possible material states that captures the stochastic nature of the MMNCs microstructure. These input samples are then passed through the predictive model to obtain corresponding outputs for the elastic modulus.

Moreover, the model is assessed for each realization of input variables. The corresponding effective elastic modulus is then obtained by passing each sampled input vector $X(i)$ with the particular values of $V_{np}^{(i)}$, $d_{np}^{(i)}$, $\varphi_o^{(i)}$, $\xi_b^{(i)}$, $\lambda_b^{(i)}$, $\eta_{int}^{(i)}$ and $V_{porosity}^{(i)}$ to the deterministic model. This is written mathematically as:

$$E_{eff,nc}^{(i)} = f(X(i)), \; i = 1, 2, 3, \dots, N \tag{17}$$

This process is repeated times for each sampled input vector. Hence, we get a set of output values for the effective elastic modulus:

$$\left\{E_{eff,nc}^{(1)}, \; E_{eff,nc}^{(2)}, \dots, \; E_{eff,nc}^{(N)}\right\} \tag{18}$$

The set of these output values represents the empirical distribution of the elastic modulus. It covers the whole range of possible outcomes under the uncertainty related to the microstructural characteristics of the material. This step is important in the transition from a deterministic estimate to a statistically informed prediction of MMNC performance.

Then statistical descriptors are extracted from the set of simulated elastic modulus values to summarize and interpret the results. The first one is the mean value, which presents the central tendency of the elastic modulus. It is calculated as the arithmetic mean of all the *N* simulated values:

$$E\left[E_{eff,nc}\right] \approx \underline{E} = \frac{1}{N}\sum_{i=1}^{N} E_{eff,nc}^{(i)} \tag{19}$$

The spread or variability in the elastic modulus is then quantified using the variance and standard deviation. The variance of effective modulus is evaluated as:

$$Var\left(E_{eff,nc}\right) \approx \frac{1}{N-1}\sum_{i=1}^{N}\left(E_{eff,nc}^{(i)} - \underline{E}\right)^2 \tag{20}$$

The standard deviation is then the square root of the variance:

$$\sigma_{E_{eff,nc}} = \sqrt{Var\left(E_{eff,nc}\right)} \tag{21}$$

The values give an idea about the uniformity of the modulus predictions across all the samples. In order to further assess the reliability of the results, confidence intervals (CI) were calculated. If the distribution of the output of $E_{eff,nc}$ is close to a normal distribution, then the 100(1−α)% confidence interval for the mean can be estimated by using:

$$CI_{1-\alpha} = \underline{E} \pm z_{\alpha}/2.\frac{\sigma_{E_{eff,nc}}}{\sqrt{N}} \tag{22}$$

where, $z_{\alpha}/2$ is the Z-score for the desired confidence level (e.g., $z_{0.025}$ = 1.96 for a 95% CI). This interval is an estimate of the range in which the true average elastic modulus is expected to fall, with a statistical support that accounts for all of the modeled uncertainties.

Furthermore, the derived distribution of $E_{eff,nc}$ could be investigated for estimating percentiles, risk thresholds, or the probability that the modulus will fall below a critical value and this information is critical for reliability assessment in engineering design. Data-driven perspective to improve the accuracy and credibility of predictive modeling under microstructural variability.

3.2 Model Sensitivity Analysis

The relationship between input and output parameters defines the reliability boundaries of the model. Measurement errors and a lack of understanding of physical processes can distort the data, leading to either an underestimation or overestimation of the elastic modulus. Sensitivity analysis, whether local or global, helps in understanding the robustness of the elastic modulus model and establishes the bounds on microstructural parameters. A local analysis examines the sensitivity of individual parameters, while a global analysis evaluates sensitivity across the entire parameter distribution. Various methods are available to assess the sensitivity of microstructural parameters (Tevatia & Srivastava, 2018; Tevatia et al., 2015). The sensitivity analysis of a single parameter (one at a time) was conducted by partial derivatives (Hamby, 1995), variations in the standard deviation of input (±SD) (Hamby, 1995), and a sensitivity index (SI) (Cacuci et al., 2005). Hamby (1995) evaluated 14 different sensitivity indices for a single output model, commonly referred to as the important index, partial rank correlation coefficient, relative index deviation,

among others. Pannell (1997) proposed a straightforward sensitivity approach that correlates the effect of multiple input parameters with a single output parameter. Recently, Tevatia & Srivastava (2018) and Tevatia et al. (2015) investigated the sensitivity of the microstructural characteristics of the MMCs in predicting fatigue crack growth life.

In the present study, eight input parameters are considered: (i) ζ, (ii) a, (iii) d_{np}, (iv) ϕ, (v) $V_{porosity}$, (vi) V_{np}, (vii) λ_b and (viii) ξ_b. Each parameter is adjusted within ±10% of its average value (**Table 1**), while the other inputs remain fixed at their mean levels. These deviations measure the impact of each parameter on the elastic modulus of Al-MMNCs, thereby defining the model's sensitivity range.

4. Results and Discussion

Here we present a comprehensive probabilistic framework for the prediction of the elastic modulus of MMNCs that systematically incorporates the critical microstructural inhomogeneities, namely porosity and nanoparticle agglomeration, into the modeling architecture. In order to facilitate transparent evaluation and reproducibility, the comprehensive material and modeling parameters are listed in **Table 2**. The prediction approach is based on statistically derived degradation factors and a stochastic parameter to successfully capture the empirical variability in matrix-reinforcement.

The validation of the proposed framework with experimental data and the existing micromechanical models confirms the superiority of the proposed framework in terms of accuracy especially in the low reinforcement fraction regime where the microstructural effects are more prominent. Each representative heterogeneity is modeled by physically grounded formulations: porosity is modeled by an exponential degradation function that captures stiffness reductions due to void-induced stress amplification and matrix discontinuities; agglomeration is quantitatively analyzed by a dual-region approach that separates uniformly dispersed from clustered nanoparticles, revealing spatial reinforcement variability and rigorously quantifying the effect of partial load transfer across imperfect matrix-particle interfaces.

A global sensitivity analysis systematically quantifies the effect of microstructure and modeling parameters on the stiffness predictions, identifying dominant sources of uncertainty and providing clear guidelines to optimize both material design and fabrication processes. Such a probabilistic modeling approach together provides an advanced and reliable tool to predict the mechanical performance in the presence of the intrinsic variabilities of industrial manufacturing, thus facilitating the rational design and application of MMNCs under operational conditions.

Table 2. Mechanical properties for the different types of MMNCs.

Parameters of MMNCs	Definition	Al-SiC	Al-Al_2O_3	Al-(L12) Al_3Ti	Al7075-TiB_2
E_m (GPa)	Elastic modulus of the matrix material	67.34	67.34	70	72
E_p (GPa)	Elastic modulus of reinforcement particles	417	400	216	410
ζ	Nanoparticle size-efficiency coefficient	0.25	0.25	0.25	0.25
a	Particle-size sensitivity exponent	0.35	0.35	0.35	0.35
d_p (nm)	Nanoparticle diameter	50	13	20	400
∅	Porosity degradation parameter	1.943	1.943	1.943	1.943
$V_{porosity}$	Porosity volume fraction	0.01	0.01	0.01	0.01
Reference		Ceschini et al. (2017), Gupta et al. (2022)	Ceschini et al. (2017), Gupta et al. (2022)	Ceschini et al. (2017), Nayak et al. (2010)	Ceschini et al. (2017), Sahoo et al. (2021)

4.1 Effectiveness of Elastic Modulus Model

To critically assess the performance of the proposed model (Equation (5)), a comprehensive comparison was carried out against a group of existing models reported in the literature (Baxter & Robinson, 2011; Hassan & Gupta, 2004; Hsu et al., 2006; Mortazavi et al., 2013; Nayak et al., 2010; Snipes et al., 2011). The primary validation benchmark is the experimentally measured elastic modulus of Al-Al_2O_3 composites. **Figure 3a** presents the performance of several predictive models (Baxter & Robinson, 2011; Hassan & Gupta, 2004; Hsu et al., 2006; Mortazavi et al., 2013; Nayak et al., 2010; Snipes et al., 2011; Mital et al., 1997; Hassanzadeh-Aghdam et al., 2018) for Al_2O_3 nanoparticles (d_{np}~50 nm) in Al matrix. The exact model parameters used in Equation (5) are provided in **Table 1**. The elastic moduli predicted by the present model are in good agreement with the experimental data especially at a nanoparticle volume fraction of 0.22%. In contrast, the majority of the existing models systematically underestimate this property, except the model of Hassanzadeh-Aghdam et al. (2018) and the framework presented herein. The systematic underestimation is mainly due to their lack of knowledge of significant phenomena such as particle size effects and porosity. **Figure 3b**, which presents the predicted elastic modulus trends for a variety of MMNC compositions in **Table 1**, can provide more insights. The elastic modulus increase with increasing nanoparticle volume fractions is clearly visible. This is consistent with previous experimental studies pointing out the large variability induced by surface defects and microstructure heterogeneity (Sahoo et al., 2021). Specifically, the presence of porosity in the MMNC microstructure has a significant negative effect on the elastic modulus due to stress concentration at the tips of the pores which facilitates void coalescence and fracture propagation under load (Yazdabadi et al., 2013; Sahoo et al., 2021).

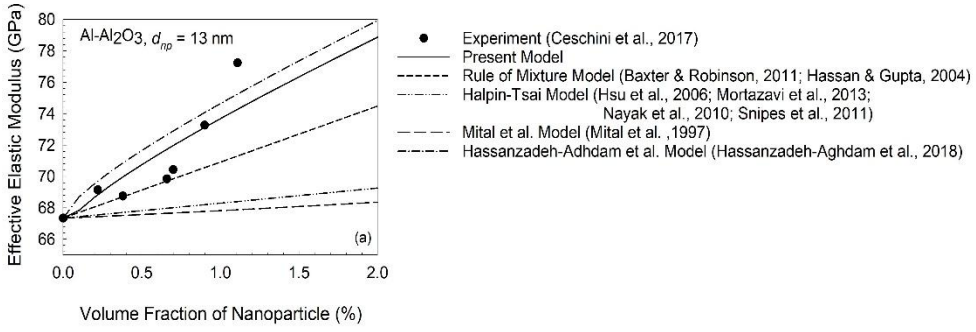

(a)

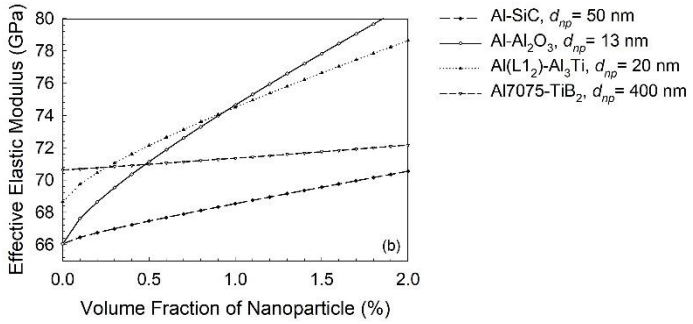

(b)

Figure 3. Comparison of present analytical elastic modulus model with (a) different models (b) various MMNCs.

This rigorous validation and parametric study highlight the importance of microstructural heterogeneities in governing the mechanical response and the need for their explicit consideration for predictive accuracy in modeling the MMNC elastic modulus.

The physical validity of the proposed agglomeration based model was evaluated by comparing the predictions with the classical Voigt, Reuss and Hashin-Shtrikman (HS) bounds. The Voigt (iso-strain) and Reuss (iso-stress) bounds give the theoretical upper and lower bounds for ideal two-phase composites and the HS bounds give the most accurate bounds for isotropic materials. These bounds were computed using matrix and particle properties at a particle volume fraction of $V_p = 0.025$ for various MMNCs as shown in **Table 3**. For example, in the Al-SiC system, the Voigt and Reuss bounds were found to be 76.08 and 68.78 GPa, respectively, and the Hashin-Shtrikman bounds were found to be between 71 and 74 GPa.

The predicted modulus by the present model is between the Voigt-Reuss bounds and close to the Reuss lower bound. This observation implies that the composite response approaches iso-stress conditions. This is physically consistent with the presence of agglomeration and non-uniform dispersion of particles. The small difference from the Hashin-Shtrikman lower bound can be explained by the effects of porosity and clustering which are explicitly included in the model and are not included in classical homogenization theories."

Table 3. Voigt-Reuss-Hashin-Shtrikman bounds for MMNCs (V_{np} = 0.025).

MMNCs	Reuss (GPa)	HS Lower (GPa)	HS Upper (GPa)	Voigt (GPa)
Al-SiC	68.78	71.23	74.44	76.08
Al-Al_2O_3	68.77	71.15	74.12	75.66
Al-Al_3Ti	71.20	72.49	73.17	73.65
Al7075-TiB_2	73.52	75.98	78.91	80.45

4.2 Effect of Porosity

Figure 4 shows the effects of porosity ($V_{porosity}$), nanoparticle volume fraction (V_{np}) and particle size (d_{np}) on the elastic modulus (E_{nc}) of Al-Al_2O_3 MMNCs. It is evident that the modulus decreases significantly with an increase in porosity from 0% to 5%. This demonstrates the negative effect of voids in reducing the stiffness by creating stress concentrations and disturbing the load transfer paths (Hassan & Gupta, 2004; Hassanzadeh-Aghdam et al., 2018; Sahoo et al., 2021). The increase in modulus values with increase in volume fractions of the nanoparticles is observed for all levels of porosity, confirming the reinforcing effect of Al_2O_3 nanoparticles by means of better load sharing between matrix and reinforcement (Hassan & Gupta, 2004; Hassanzadeh-Aghdam et al., 2018; Sahoo et al., 2021).

The results are also strongly dependent on the size of the nanoparticle. The larger the particle size the lower are the modulus values for a given porosity and volume fraction. This is due to the decreased surface to volume ratio which results in a reduction in the effective bonding area and limits the stress transfer efficiency (Hassan & Gupta, 2004; Hassanzadeh-Aghdam et al., 2018; Sahoo et al., 2021). The synergistic effects show that the optimal stiffness can be achieved with low porosity, small nanoparticle size and high nanoparticle loadings whereas presence of high porosity and large particle size significantly lowers the modulus. The obtained results are in accordance with the micromechanical theory and previous experimental results for MMNC systems (Hassan & Gupta, 2004; Hassanzadeh-Aghdam et al., 2018; Sahoo et al., 2021).

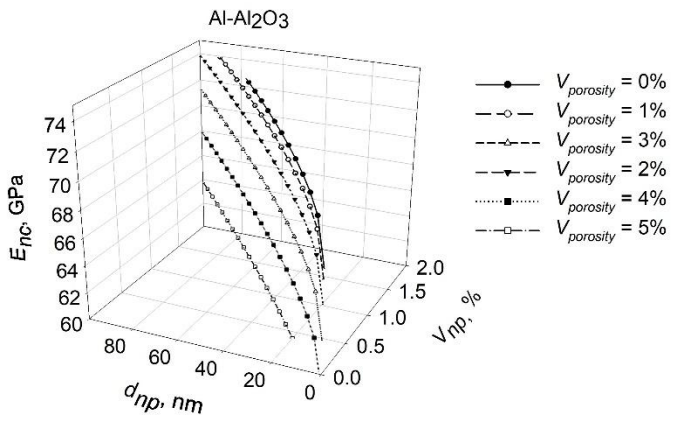

Figure 4. Effect of porosity ($V_{porosity}$), % on elastic modulus (E_{nc}), GPa of Al-Al_2O_3 MMNCs with combined effect of V_{np} & d_{np}

To validate the proposed porosity degradation factor, the model predictions were benchmarked against classical porous-solid relations. For comparison, the Mackenzie model for spherical pores predicts a quadratic dependence of stiffness on porosity, given by $E/E_0 = 1 - 1.9P + 0.9P^2$, while the Phani-Niyogi model expresses the reduction as $E/E_0 = (1 - P)^n$, where the exponent n depends on pore morphology.

For the low porosity level considered in this study ($P = 0.01$), both models reduce to a first-order approximation of the form $E/E_0 \approx 1 - CP$, with $C \approx 1.5$-2 for spherical pores. The linear degradation term adopted in the present model is therefore consistent with these classical relations in the dilute porosity regime. Furthermore, the calibration parameter ϕ implicitly captures the influence of pore morphology and distribution. For spherical pores, the model reproduces trends consistent with $n \approx 2$, while for non-spherical or irregular pores, the effective reduction becomes stronger, consistent with higher exponents reported in the Phani-Niyogi model.

The porosity parameter ϕ was treated as an effective morphology-dependent degradation coefficient representing the average influence of porosity on elastic modulus reduction. No direct three-dimensional pore characterization (e.g., micro-CT tomography) was available for the investigated MMNC systems. Within the investigated dilute porosity regime ($V_{porosity} \leq 0.05$), sensitivity analysis showed that reasonable variations in ϕ produced only moderate changes in elastic modulus predictions (approximately 2-6%), indicating that the proposed framework is reasonably robust to pore morphology assumptions.

This comparison demonstrates that the proposed porosity formulation is physically consistent with established porous-solid theories while retaining the flexibility to account for microstructural features such as pore shape, clustering, and non-uniform distribution.

4.3 Agglomerated State of Nanoparticles in the Metal Matrix

One of the critical issues that influences microstructural changes and mechanical response of MMNCs is the agglomeration of the nanoparticles. The high surface energy of the nanoparticles can cause them to stick together easily during processing and form composites with heterogeneous spatial distributions that can have an important effect on the behavior of the composite. Finally, the quantitative effect of agglomeration on the effective elastic modulus ($E_{agg,nc}$) of Al-Al_2O_3 MMNCs studied is presented in **Figure 5** for a fixed

nanoparticle volume fraction and size parameters. The two basic variables that describe agglomeration are the volume fraction of matrix that contains agglomerated regions: ξ_b and the fraction of the total nanoparticles that are trapped in the agglomerated regions: λ_b. The condition schematically is by ξ_b=1, represents that entire domain is agglomerated (fully clustered system) and homogeneous dispersion corresponds to: $\xi_b \to 0$, $\lambda_b \to 0$ shown in **Figure 1b** Note that the case of $\xi_b = \lambda_b$ corresponds to the uniform dispersion of nanoparticles and provides a reference elastic modulus $E_{agg,nc}$. Agglomerated clusters lead to large microstructural discontinuities and stress field, which can negatively impact load transfer mechanisms and cause sites in which premature crack initiation and propagation can occur (Boostani et al., 2016; Liu & Bian, 2018). These defect related phenomena result in measurable decrease in the stiffness of the composite, and decrease the durability and reliability of MMNCs as demonstrated in various experimental and computational studies (Golbang et al., 2017; Karevan et al., 2010; Pan & Bian, 2017; Pouyanmehr et al., 2022; Qiao et al., 2011; Shi et al., 2004). This is a reminder of the need to carefully control the dispersion of the nanoparticles as part of the synthesis protocol and extract the optimum of the intrinsic mechanical properties of the MMNCs.

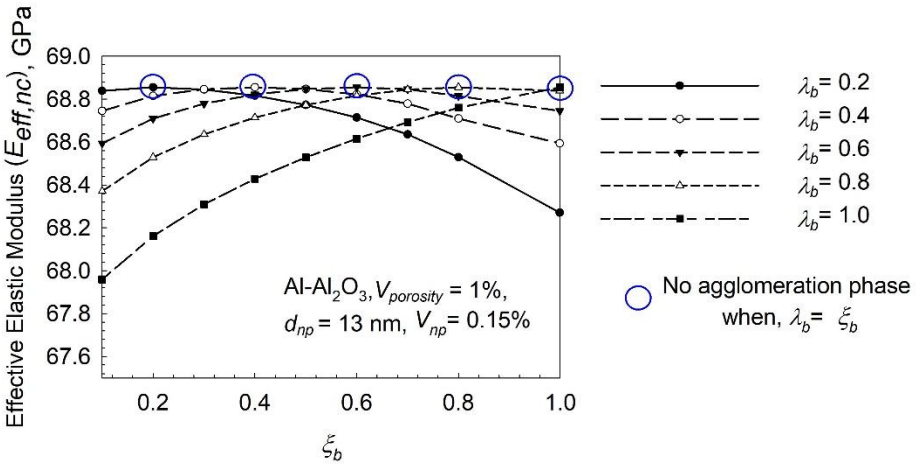

Figure 5. Effect of agglomeration in Al-Al_2O_3 MMNCs.

In the extreme scenario of complete nanoparticle agglomeration ($\lambda_b = 1$), all nanoparticles merge into distinct, spherical clusters, thereby eliminating their uniform distribution within the metal matrix. The interaction between nanoparticle volume fraction V_{np} and diameter d_{np} under this condition is illustrated in **Figure 6**. These findings confirm that both increased particle loading and decreased particle size are essential for mitigating stiffness degradation in cases of non-ideal dispersion. For a constant V_{np}, decreasing ξ_b the volumetric fraction of the matrix containing agglomerates precipitates a marked diminution in the effective elastic modulus $E_{agg,nc}$. This decrease is mainly due to the reduced involvement of clustered particles in load transfer processes, which is caused by a limited interfacial contact area and the presence of voids typical of clustering (Boostani et al., 2016; Liu & Bian, 2018). Additionally, in agglomerated conditions, there is an inverse relationship with the increasing size of nanoparticles, highlighting the advantage of smaller nanoparticles in improving elastic stiffness due to their naturally higher surface-to-volume ratios and more effective interfacial bonding (Chen et al., 2018; Pouyanmehr et al., 2022).

The dependence of the reinforcement effects on the particle size in particulate composites can be studied by micromechanics-based homogenization frameworks like the modified Mori-Tanaka schemes. These

frameworks involve interfacial stress, surface energy, and particle interactions. These approaches provide a mechanistic insight into the behavior of the nanoscale considering interfacial fields, non-dilute interactions and eigenstrain. However, they require complex analyses and detailed interfacial parameters which are not always readily available. In the present model, the size-efficiency factor, φ_o, is used as a phenomenological parameter to describe the effect of particle size on the efficiency of load transfer. Although this is a semi-empirical approach, it is a computationally efficient and interpretable way of including nanoscale effects in a continuum framework. The proposed formulation offers a good balance between model accuracy and analytical tractability for engineering applications.

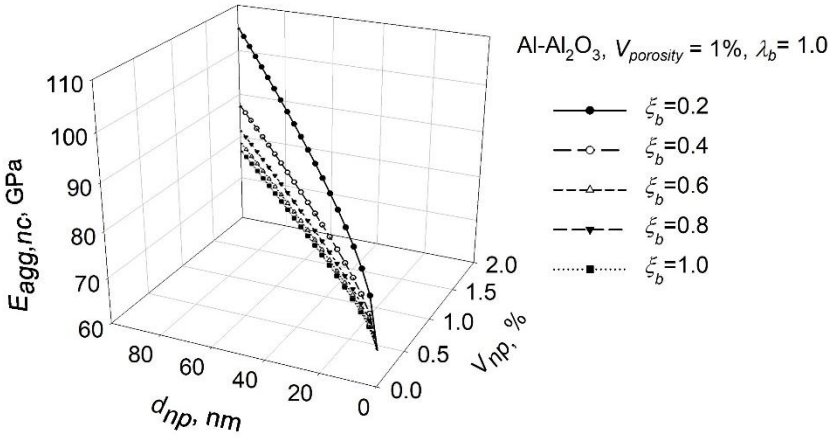

Figure 6. Impact of complete nanoparticle agglomeration ($\lambda_b = 1$) on elastic modulus (E_{nc}), GPa of Al-Al_2O_3 MMNCs as a function of nanoparticle volume fraction (V_{np}), % and (d_{np}), nm.

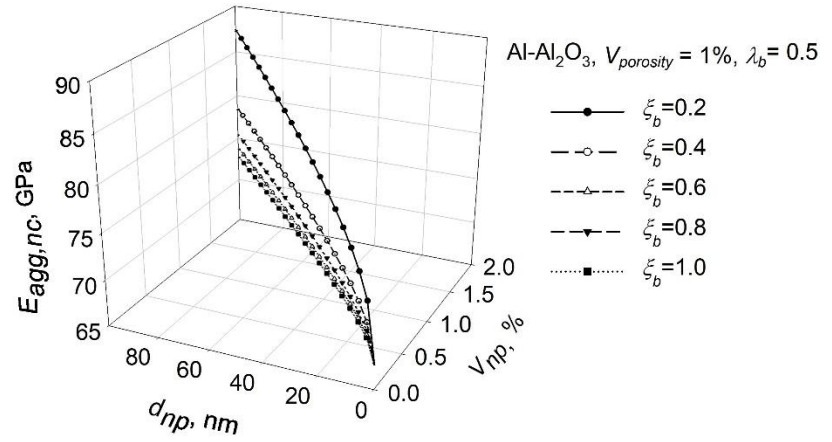

Figure 7. Effect of nanoparticle complete partial agglomeration ($\lambda_b = 0.5$) on elastic modulus (E_{nc}), GPa of Al-Al_2O_3 MMNCs with volume fraction of nanoparticles (V_{np}), % and nanoparticle diameter (d_{np}), nm as a parameter.

4.4 Probabilistic Analysis of Effective Elastic Modulus

The contribution of microstructural variability is presented here in terms of probabilistic models of the effective elastic modulus (E_{eff}) of Al-Al_2O_3 MMNCs. The histogram of the modulus values from Monte

Carlo simulations, with a kernel density estimate superposed, is presented in **Figure 8a**. The statistical convergence of the study was 10,000 Monte Carlo simulation trials. The results of the analysis of convergence showed that the convergence is stable in the 5000 sample number, and the relative change (< 1%) of the mean effective elastic modulus was calculated. Further, the smaller the sample size, the smaller the standard error of the mean; and the standard error of mean was small enough at 10,000 sample sizes to ensure reliable output statistics. This sample size is the "right" balance of calculation and precision. The average value of these results is ~43.9 GPa, slightly biased towards lower stiffness values. The reason for this asymmetry is the lognormal behavior of the porosity that more than compensates the increase in the void fractions and consequently reduces the stiffness. This is distinct from models that are deterministic, that give one point estimate. The drawbacks of the probabilistic approach are that it incorporates the whole statistical spectrum of possible outcomes, reflecting the natural variability caused by the porosity and agglomeration. The spread measured here is similar with that reported from experimental works published elsewhere, where experimentally measured elastic modulus value results are sometimes lower than the theoretical value because defects created on the production.

The empirical cumulative distribution function (ECDF) shown in **Figure 8b** gives the percentage of time that performance is not below a certain threshold. This plot shows the probability of being less than a certain value, with a probability of being less than 42 GPa of about 10%, and less than 45.5 GPa of about 90%. The ECDF gives an immediate risk-based interpretation: If for example, the minimum required value for the stiffness of a design is 44.5 Gpa, nearly 30% of its realizations would fail the design requirement. The ECDF allows the engineer to convert modulus predictions into similar terms of cumulative probability to allow setting of confidence-based safety margins, particularly when demanding reliability-sensitive applications. Three reliabilities are shown to give translations of the notions between the probabilistic and practical engineering context in **Figure 8c**: the reliability curve. Assuming that the requirements are conservative, around 42 GPa, the probability of failure will be very small. But as soon as the required modulus reaches about 46 GPa, the failure probability goes up to about 65%. The steep non-linear increase accentuates the increased risk of under-performance in designing close to the mean modulus. The curve shows the need for a reliability-based approach to design; an approach in which one imposes limits on the design that are commensurate with the risk that one is willing to take, reasonable limits are assumed to lie at or below the 5th percentile of the modulus distribution.

Together the three visualizations give a comprehensive assessment of the uncertainty in the output. The distribution provides a measure of overall spread, the ECDF shows the cumulative probability at different levels, and the reliability curve links directly the material variability with the risk of failure. These findings illustrate that besides their impact on the average modulus, these microstructural faults tend to promote variability, requiring statistical modelling for the design of reliable structures. The key advantage of the present is the incorporation of the uncertainty thus making the present model-based tool for prediction more reliable than conventional deterministic model approaches for challenging structural applications for MMNCs. The predictive property of the proposed model was evaluated with some representative experimental data sets from literature on MMNC systems. Comparison showed the root mean square error (RMSE) of 2.10 GPa and the mean absolute percentage error (MAPE) of 2.81%, proving there was good agreement between the elastic modulus values predicted and experimental. The small error values shown suggest the ability of the simplified formulation to capture the impact of the agglomeration and porosity on the stiffness.

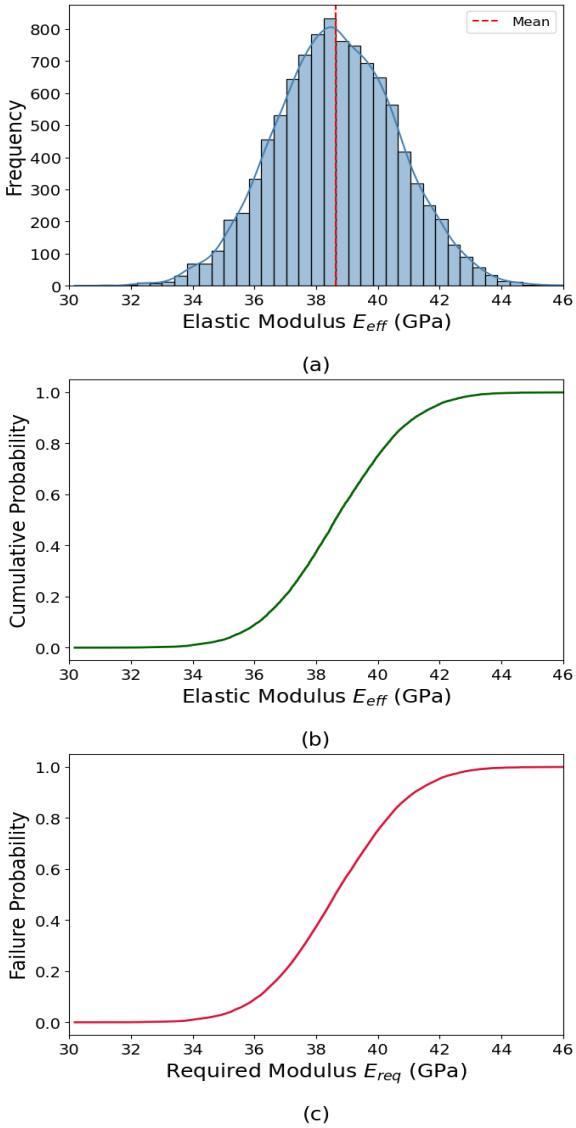

Figure 8. Probabilistic analysis of the effective elastic modulus (E_{eff}) of Al-Al_2O_3 MMNCs: (a) histogram with KDE showing distribution shape, (b) ECDF quantifying cumulative probability, and (c) reliability curve linking modulus variability to failure probability.

4.5 Sensitivity Analysis

A detailed sensitivity analysis was undertaken to quantify the effect that individual microstructural parameters have on the elastic modulus of Al–Al_2O_3 MMNCs. The impact of each parameter was studied by varying its value by ±10% and fixing all other parameters. The parameters analyzed were ζ, a, d_{np}, ϕ, $V_{porosity}$, V_{np}, λ_b, and ξ_b. Variations of elastic modules obtained were synthesized and visualized by making use of spider plot of various sensitivities as shown in **Figure 9**. Especially the parameter ζ gave a range of –0.40% to +0.60%, and the parameter a gave a more significant change to the modulus of the range from –0.82% and +0.90%. The impact was more modest for parameter d_{np} was, with values from -

0.21% to +0.23% different. This was almost equally true of parameter ϕ, which varied between -0.20% and +0.19%. Similarly, the deviations of the parameters $V_{porosity}$ and V_{np} were about ±0.19 % and ±0.35 % respectively. In contrast, λ_b and ξ_b added relatively little, and had variations of –0.38% to +0.37% and –0.35% to +0.41% respectively. These observations collectively show that the main sensitivities ζ, a, λ_b, and ξ_b have a greater influence on the elastic modulus prediction of MMNCs than d_{np}, ϕ, $V_{porosity}$ and V_{np}. In the parameter space shown in **Figure 9**, the main regulators of stiffness are the agglomeration-related and the geometrical parameters and dominate over the effect of porosity and size of the particles.

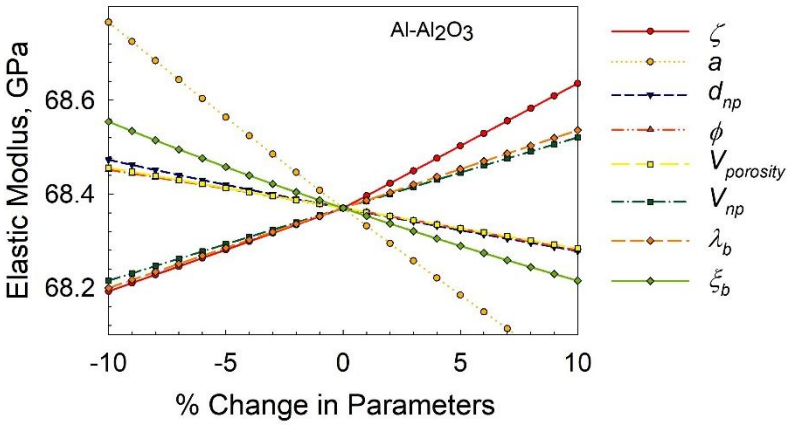

Figure 9. The sensitivity analysis using the various modeling parameters (ζ, a, d_{np}, ϕ, $V_{porosity}$, V_{np}, λ_b and ξ_b) on the elastic modulus (E_{nc}) of Al-Al_2O_3 MMNCs.

5. Conclusions

By combining in a single framework micromechanical modeling, experimental correlations and probabilistic approaches, this work offers a comprehensive and systematic investigation on the complex impact of porosity, and nanoparticle agglomeration on the elastic modulus of MMNCs. The key findings include:

(1) A new predictive model has been developed which quantifies the elastic modulus of MMNCs that readily accounts for the impact of porosity and clustering of nanoparticles. This framework uses probabilistic approaches, not deterministic approaches, to abstract the inherent variations in the phenomenon being modelled and greatly improves the robustness and reliability of performance evaluations.

(2) The influence of the microstructural voids is significant on the stiffness, reducing with the increase of porosity the elastic modulus significantly. These blemishes are stress concentration points and decrease effective load transfer and mechanical strength of the composite.

(3) The formation of nanoparticulate agglomerates causes a reduction in the efficiency of load transfer between the parts, stress localization, and, as a result, significant reduction in the rigidity and mechanical robustness of the system. This salient measurement demonstrates the fact that it is significant to control the spread of the particles in the matrix in order to maximize reinforcing effects.

(4) The improved accuracy and predictive capability of the proposed framework is verified by comparison with available theoretical models and experimental results, and hence the framework is reliable for a number of regimes of microstructures.

(5) The probabilistic analysis provides a nuanced insight into the model outputs' uncertainties and the failure probability by using histogram output distributions, ECDFs and reliability curves.

(6) Sensitivity analyses suggest that the sensitivities of the elastic modulus are dominated by the parameters ζ, a, λ_b, and ξ_b, and hence have particular significance in the control of the process and improvement of the model. Furthermore, it is found that the parameters d_{np}, , ϕ, $V_{porosity}$ and V_{np} have relatively lower influences and guiding the prioritization of experimental/ computational efforts.

The proposed model is a prediction model of the elastic modulus of MMNCs, based on microstructural parameters, using a stochastic approach to take into consideration the variability of the material. Uses Monte Carlo simulations to provide a probability distribution on the elastic modulus, not available from a deterministic approach. The environmental and load conditions are not explicitly modelled but can be implicitly modelled by modifications of the distribution of the input parameters. The model can be readily adapted to include parameters including temperature dependence and is numerically efficient, making it a highly successful prediction model based on microstructure of the elastic properties. To sum up, this contribution develops the state of the art in MMNC modeling including the incorporation of microstructural features into the modeling and prediction from a probabilistic perspective, leading to improved predictability from deterministic estimates to uncertainty-informed predictions. This paradigm shift opens the door to an optimized design of nanocomposites for critical engineering applications that will provide reliability for their efficient use, safety and longevity in real time.

Conflicts of Interest

The authors state that there are no conflicts of interest related to the publication of this manuscript.

Acknowledgments

The authors extend their gratitude to all individuals and institutions that supported this work. They sincerely acknowledge any assistance received during the preparation of this manuscript.

AI Disclosure

During the preparation of this work, the author used generative AI in order to improve the language of the article. After using this tool/service, the author reviewed and edited the content as needed and takes full responsibility for the content of the publication.

References

Abdizadeh, H., Ebrahimifard, R., & Baghchesara, M.A. (2014). Investigation of microstructure and mechanical properties of nano MgO reinforced Al composites manufactured by stir casting and powder metallurgy methods: a comparative study. *Composites Part B: Engineering*, *56*, 217-221.

Ahmad, S.N., Hashim, J., & Ghazali, M.I. (2005). The effects of porosity on mechanical properties of cast discontinuous reinforced metal- matrix composite. *Journal of Composite Materials*, *39*(5), 451-466. https://doi.org/10.1177/0021998305047096

Ahmad, S.N., Hashim, J., & Ghazali, M.I. (2007). Effect of porosity on tensile properties of cast particle reinforced MMC. *Journal of Composite Materials*, *41*(5), 575-589. https://doi.org/10.1177/0021998306066720

Altarabsheh, I., Altarabsheh, A., & Chen, X. (2025). Probabilistic prediction of stress-strain curves at the nanoscale: A multi-output Gaussian process approach with molecular dynamics simulations. *Journal of Applied Physics*, *137*(22), 224304. https://doi.org/10.1063/5.0250014

Baxter, S.C., & Robinson, C.T. (2011). Pseudo-percolation: critical volume fractions and mechanical percolation in polymer nanocomposites. *Composites Science and Technology*, *71*(10), 1273-1279. https://doi.org/10.1016/j.compscitech.2011.04.010

Boostani, A.F., Taherzadeh Mousavian, R., Tahamtan, S., Yazdani, S., Azari Khosroshahi, R., Wei, D., Xu, J., Zhang, X., & Jiang, Z.Y. (2016). Solvothermal-assisted graphene encapsulation of SiC nanoparticles: a new horizon toward toughening aluminium matrix nanocomposites. *Materials Science and Engineering: A*, *653*, 99-107. https://doi.org/10.1016/j.msea.2015.12.008

Brassell, G.W., Horak, J.A., & Butler, B.L. (1975). Effects of porosity on strength of carbon-carbon composites. *Journal of Composite Materials*, *9*(3), 288-296.

Cacuci, D.G., Ionescu-Bujor, M., & Navon, I.M. (2005). *Sensitivity and uncertainty analysis, volume II: applications to large-scale systems*. CRC press, Boca Raton.

Ceschini, L., Dahle, A., Gupta, M., Jarfors, A.E.W., Jayalakshmi, S., Morri, A., Rotundo, F., & Toschi, S. (2017). *Aluminum and Magnesium Metal Matrix Nanocomposites* (pp. 19-20). Springer, Singapore.

Chen, S., Hassanzadeh-Aghdam, M.K., & Ansari, R. (2018). An analytical model for elastic modulus calculation of SiC whisker-reinforced hybrid metal matrix nanocomposite containing SiC nanoparticles. *Journal of Alloys and Compounds*, *767*, 632-641. https://doi.org/10.1016/j.jallcom.2018.07.102

Dahiya, M., Khanna, V., & Bansal, S.A. (2023). Aluminium-graphene metal matrix nanocomposites: modelling, analysis, and simulation approach to estimate mechanical properties. *Materials Today: Proceedings*, *78*, 414-419. https://doi.org/10.1016/j.matpr.2022.10.181

El-Kady, O., & Fathy, A. (2014). Effect of SiC particle size on the physical and mechanical properties of extruded Al matrix nanocomposites. *Materials and Design*, *54*, 348-353. https://doi.org/10.1016/j.matdes.2013.08.049

Engelstad, S.P., & Reddy, J.N. (1994). Probabilistic methods for the analysis of metal-matrix composites. *Composites Science and Technology*, *50*(1), 91-107. https://doi.org/10.1016/0266-3538(94)90129-5

Golbang, A., Famili, M.H.N., & Shirvan, M.M.M. (2017). A method for quantitative characterization of agglomeration degree in nanocomposites. *Composites Science and Technology*, *145*, 181-186. https://doi.org/10.1016/j.compscitech.2017.04.013

Gupta, M., & Wong, W.L.E. (2015). Magnesium-based nanocomposites: Lightweight materials of the future. *Materials Characterization*, *105*, 30-46. https://doi.org/10.1016/j.matchar.2015.04.015

Gupta, S., Tevatia, A., & Rana, K.P.S. (2022). A fatigue crack growth life prediction model for metal matrix nanocomposites: contribution of strengthening factors. *Advanced Composite Materials*, *31*(1), 43-61.

Gupta, S., Tevatia, A., & Rana, K.P.S. (2025). Predictive modeling and sensitivity analysis for averting nanoparticle agglomeration in metal matrices. *Defence Science Journal*, *75*(4), 451-462. https://doi.org/10.14429/dsj.20407

Hamby, D.M. (1995). A comparison of sensitivity analysis techniques. *Health Physics*, *68*(2), 195-204.

Hassan, S.F., & Gupta, M. (2004). Development of high performance magnesium nanocomposites using solidification processing route. *Materials Science and Technology*, *20*(11), 1383-1388. https://doi.org/10.1179/026708304X3980

Hassan, S.F., & Gupta, M. (2006). Effect of length scale of Al_2O_3 particulates on microstructural and tensile properties of elemental Mg. *Materials Science and Engineering: A*, *425*(1-2), 22-27. https://doi.org/10.1016/j.msea.2006.03.029

Hassanzadeh-Aghdam, M.K., Mahmoodi, M.J., & Ansari, R. (2018). A comprehensive predicting model for thermomechanical properties of particulate metal matrix nanocomposites. *Journal of Alloys and Compounds*, *739*, 164-177. https://doi.org/10.1016/j.jallcom.2017.12.232

He, F., Han, Q., & Jackson, M.J. (2008). Nanoparticulate reinforced metal matrix nanocomposites–a review. *International Journal of Nanoparticles*, *1*(4), 301-309.

Hsu, C.J., Chang, C.Y., Kao, P.W., Ho, N.J., & Chang, C.P. (2006). Al-Al3Ti nanocomposites produced in situ by friction stir processing. *Acta Materialia*, *54*(19), 5241-5249. https://doi.org/10.1016/j.actamat.2006.06.054

Karevan, M., Pucha, R.V., Bhuiyan, Md. A., & Kalaitzidou, K. (2010). Effect of interphase modulus and nanofiller agglomeration on the tensile modulus of graphite nanoplatelets and carbon nanotube reinforced polypropylene nanocomposites. *Carbon Letters*, *11*(4), 325-331. https://doi.org/10.5714/cl.2010.11.4.325

Liu, W., & Bian, L. (2018). Influences of inclusions and corresponding interphase on elastic properties of composites. *Archive of Applied Mechanics*, *88*(9), 1507-1524. https://doi.org/10.1007/s00419-018-1384-8

Mazaheri, M., Payandehpeyman, J., & Hedayatian, M. (2024). Agglomeration and interphase-influenced effective elastic properties of Metal/Graphene nanocomposites: a developed mean-field model. *Composite Structures*, *329*, 117762. https://doi.org/10.1016/j.compstruct.2023.117762

McWilliams, B.A., Ramesh, K.T., & Yen, C.-F. (2013). Probabilistic response of heterogeneous particle reinforced metal matrix composites with particle size dependent strengthening. *Computational Materials Science*, *79*, 15-24. https://doi.org/10.1016/j.commatsci.2013.05.047

Mirza, F.A., & Chen, D.L. (2012). An analytical model for predicting the yield strength of particulate-reinforced metal matrix nanocomposites with consideration of porosity. *Nanoscience and Nanotechnology Letters*, *4*(8), 794-800.

Mital, S.K., Murthy, P.L.N., & Goldberg, R.K. (1997). Micromechanics for particulate-reinforced composites. *Mechanics of Composite Materials and Structures*, *4*(3), 251-266. https://doi.org/10.1080/10759419708945883

Molina, J.M., Prieto, R., Narciso, J., & Louis, E. (2009). The effect of porosity on the thermal conductivity of Al-12 wt.% Si/SiC composites. *Scripta Materialia*, *60*(7), 582-585. https://doi.org/10.1016/j.scriptamat.2008.12.015

Mortazavi, B., Bardon, J., & Ahzi, S. (2013). Interphase effect on the elastic and thermal conductivity response of polymer nanocomposite materials: 3D finite element study. *Computational Materials Science*, *69*, 100-106. https://doi.org/10.1016/j.commatsci.2012.11.035

Nayak, S.S., Pabi, S.K., & Murty, B.S. (2010). Al-(L12)Al3Ti nanocomposites prepared by mechanical alloying: Synthesis and mechanical properties. *Journal of Alloys and Compounds*, *492*(1-2), 128-133. https://doi.org/10.1016/j.jallcom.2009.10.274

Pan, J., & Bian, L. (2017). Influence of agglomeration parameters on carbon nanotube composites. *Acta Mechanica*, *228*(6), 2207-2217. https://doi.org/10.1007/s00707-017-1820-9

Pan, J., & Bian, L. (2019). A physics investigation for influence of carbon nanotube agglomeration on thermal properties of composites. *Materials Chemistry and Physics*, *236*, 121777. https://doi.org/10.1016/j.matchemphys.2019.121777

Pannell, D.J. (1997). Sensitivity analysis of normative economic models: theoretical framework and practical strategies. *Agricultural Economics*, *16*(2), 139-152.

Pouyanmehr, R., Hassanzadeh-Aghdam, M.K., & Ansari, R. (2022). Estimation of elastic modulus and Poisson's ratio of concrete containing graphene nanosheets: a focus on nano-filler agglomeration and hydration time. *Computational Sciences and Engineering*, *2*(1), 111-123. https://doi.org/10.22124/cse.2022.22353.1033

Qiao, R., Deng, H., Putz, K.W., & Brinson, L.C. (2011). Effect of particle agglomeration and interphase on the glass transition temperature of polymer nanocomposites. *Journal of Polymer Science, Part B: Polymer Physics*, *49*(10), 740-748. https://doi.org/10.1002/polb.22236

Rana, R.S., Purohit, R., & Das, S. (2012). Reviews on the influences of alloying elements on the microstructure and mechanical properties of aluminum alloys and aluminum alloy composites. *International Journal of Scientific and Research Publications*, *2*(6), 1-7.

Rapoff, A.J., Heisey, D.M., & Vanderby, R. (1999). A probabilistic rule of mixtures for elastic moduli. *Journal of Biomechanics*, *32*(2), 189-193. https://doi.org/10.1016/S0021-9290(98)00155-9

Sahoo, B.P., Das, D., & Chaubey, A.K. (2021). Strengthening mechanisms and modelling of mechanical properties of submicron-TiB2 particulate reinforced Al 7075 metal matrix composites. *Materials Science and Engineering: A*, *825*, 141873. https://doi.org/10.1016/j.msea.2021.141873

Shah, A.R., Murthy, P.L.N., Mital, S.K., & Bhatt, R.T. (2000). Probabilistic modeling of ceramic matrix composite strength. *Journal of Composite Materials*, *34*(8), 670-688. https://doi.org/10.1177/002199830003400803

Shi, D.L., Feng, X.Q., Huang, Y.Y., Hwang, K.C., & Gao, H. (2004). The effect of nanotube waviness and agglomeration on the elastic property of carbon nanotube-reinforced composites. *Journal of Engineering Materials and Technology*, *126*(3), 250-257. https://doi.org/10.1115/1.1751182

Sinha, A., & Farhat, Z. (2015). Effect of surface porosity on tribological properties of sintered pure Al and Al 6061. *Materials Sciences and Applications*, *6*(6), 549-566. https://doi.org/10.4236/msa.2015.66059

Snipes, J.S., Robinson, C.T., & Baxter, S.C. (2011). Effects of scale and interface on the three-dimensional micromechanics of polymer nanocomposites. *Journal of Composite Materials*, *45*(24), 2537-2546. https://doi.org/10.1177/0021998311401104

Tevatia, A., & Srivastava, S.K. (2018). The energy-based multistage fatigue crack growth life prediction model for DRMMC s. *Fatigue & Fracture of Engineering Materials & Structures*, *41*(12), 2530-2540.

Tevatia, R., Demirel, Y., Rudrappa, D., & Blum, P. (2015). Effects of thermodynamically coupled reaction diffusion in microalgae growth and lipid accumulation: Model development and stability analysis. *Computers & Chemical Engineering*, *75*, 28-39.

Yang, Z., & Meng, Z. (2026). A Review of computational modeling of polymer composites and nanocomposites. *Polymers*, *18*(4), 443. https://doi.org/10.3390/polym18040443

Yao, X., Zhang, Z., Zheng, Y.F., Kong, C., Quadir, M.Z., Liang, J.M., Chen, Y.H., Munroe, P., & Zhang, D.L. (2017). Effects of SiC nanoparticle content on the microstructure and tensile mechanical properties of ultrafine grained AA6063-SiCnp nanocomposites fabricated by powder metallurgy. *Journal of Materials Science and Technology*, *33*(9), 1023-1030. https://doi.org/10.1016/j.jmst.2016.09.022

Yazdabadi, H.G., Ekrami, A., Kim, H.S., & Simchi, A. (2013). An investigation on the fatigue fracture of P/M Al-SiC nanocomposites. *Metallurgical and Materials Transactions A*, *44*(6), 2662-2671.

Zare, Y. (2016). Modeling the yield strength of polymer nanocomposites based upon nanoparticle agglomeration and polymer-filler interphase. *Journal of Colloid and Interface Science*, *467*, 165-169. https://doi.org/10.1016/j.jcis.2016.01.022

Zhang, W., & Xu, J. (2022). Advanced lightweight materials for automobiles: a review. *Materials & Design*, *221*, 110994. https://doi.org/10.1016/j.matdes.2022.110994

Zhao, K., Guo, R., Liu, G., & Li, Y. (2022). Monte Carlo simulation for exploring the mechanical properties of particle-reinforced composites based on the scale boundary finite element method. *Composite Structures*, *297*, 115933. https://doi.org/10.1016/j.compstruct.2022.115933

Zhong, X.L., Wong, W.L.E., & Gupta, M. (2007). Enhancing strength and ductility of magnesium by integrating it with aluminum nanoparticles. *Acta Materialia*, *55*(18), 6338-6344. https://doi.org/10.1016/j.actamat.2007.07.039